ESI for:

The Reactivity of Antimony and Bismuth *N,C,N*-Pincer Compounds toward K[BEt$_3$H] – the Formation of Heterocyclic Compounds *vs*. Element-Element Bonds *vs.* Stable Terminal Sb-H Bonds.

P. Novák, M. Erben, R. Jambor, M. Hejda, A. Růžička, E. Rychagova, S. Ketkov* and L. Dostál*

*E-mails: libor.dostal@upce.cz (L.D.), sketkov@iomc.ras.ru (S.K.)

Table of contents:

1) Synthesis and NMR spectra of starting compounds.

Synthesis of 2-Sb

779 mg (1.36 mmol) of **1-Sb** was dissolved in benzene (15 mL) and 270 μL (1.36 mmol) of neat Me_3SiCH_2OTf was added. The solution was stirred for 12 h at r.t. and the reaction mixture was evaporated. The solid residue was washed with hexane (*ca* 2x10 mL) and dried *in vacuo* giving **2-Sb** as a white powder. Yield 842 mg, 77%, m.p. 240-244 °C. Anal. Calcd for $C_{37}H_{50}F_3N_2O_3SSbSi$ (Mr = 809.72): C, 54.9 %; H, 6.2 %; N, 3.5 %. Found: C, 55.2 %; H 6.5 %; N, 3.8 %. ^{1}H NMR (500 MHz, CD_3CN): δ -0.49 [9H, s, Si(CH_3)$_3$]; 0.87 [2H, s, SiCH_2]; 1.10 [6H, d, $^3J_{H,H}$ = 6.7 Hz, *i*Pr-CH_3]; 1.21 [6H, d, $^3J_{H,H}$ = 6.9 Hz, *i*Pr-CH_3]; 1.26 [6H, d, $^3J_{H,H}$ = 6.7 Hz, *i*Pr-CH_3]; 1.29 [6H, d, $^3J_{H,H}$ = 6.9 Hz, *i*Pr-CH_3]; 2.69 [2H, h, $^3J_{H,H}$ = 6.9 Hz, *i*Pr-CH]; 3.09 [2H, h, $^3J_{H,H}$ = 6.7 Hz, *i*Pr-CH]; 7.32-7.38 [6H, m, Ar-H]; 8.08 [1H, t, $^3J_{H,H}$ = 7.7 Hz, Ar-H]; 8.47 [2H, d, $^3J_{H,H}$ = 7.7 Hz, Ar-H]; 9.16 [2H, s, CH=N] ppm. ^{13}C{^{1}H} NMR (125.76 MHz, CD_3CN): δ -0.7 [Si(CH$_3$)$_3$]; 7.9 [SiCH$_2$]; 23.7 [*i*Pr-CH_3]; 23.9 [*i*Pr-CH_3]; 25.1 [*i*Pr-CH_3]; 26.8 [*i*Pr-CH_3]; 29.1 [*i*Pr-CH]; 30.0 [*i*Pr-CH]; not detected [CF$_3$], 125.6 [Ar-C]; 125.9 [Ar-C]; 129.5 [Ar-C]; 133.3 [Ar-C]; 137.5 [Ar-C]; 140.3 [Ar-C]; 141.2 [Ar-C]; 141.4 [Ar-C]; 142.0 4 [Ar-C]; 156.3 [C-ipso]; 171.1 [CH=N] ppm.

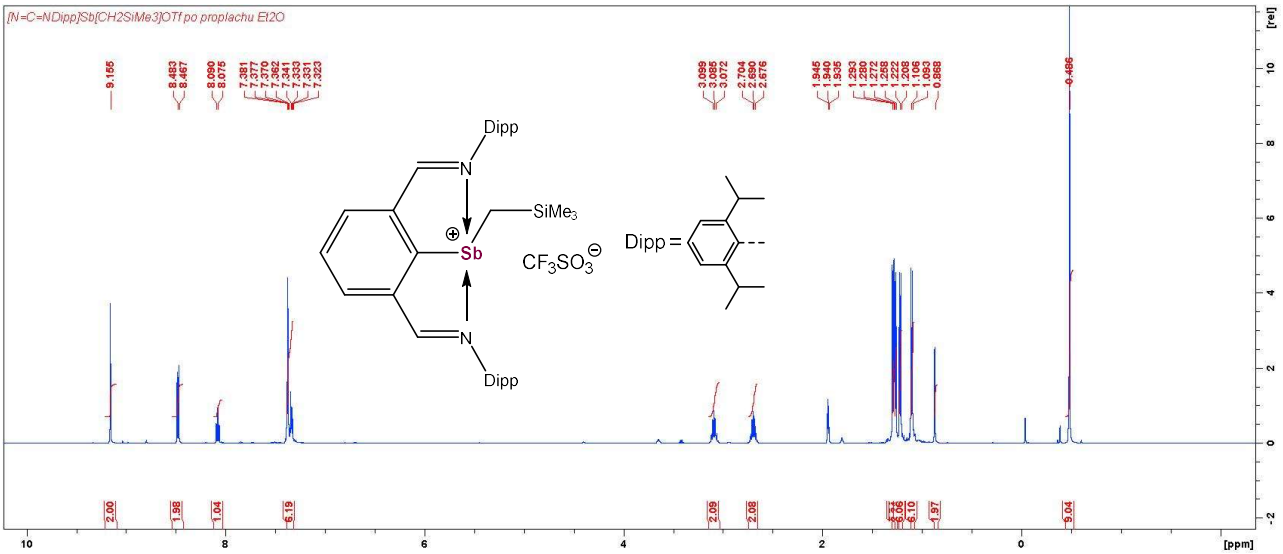

Figure S1: ^{1}H NMR spectrum of **2-Sb** in CD_3CN (500 MHz).

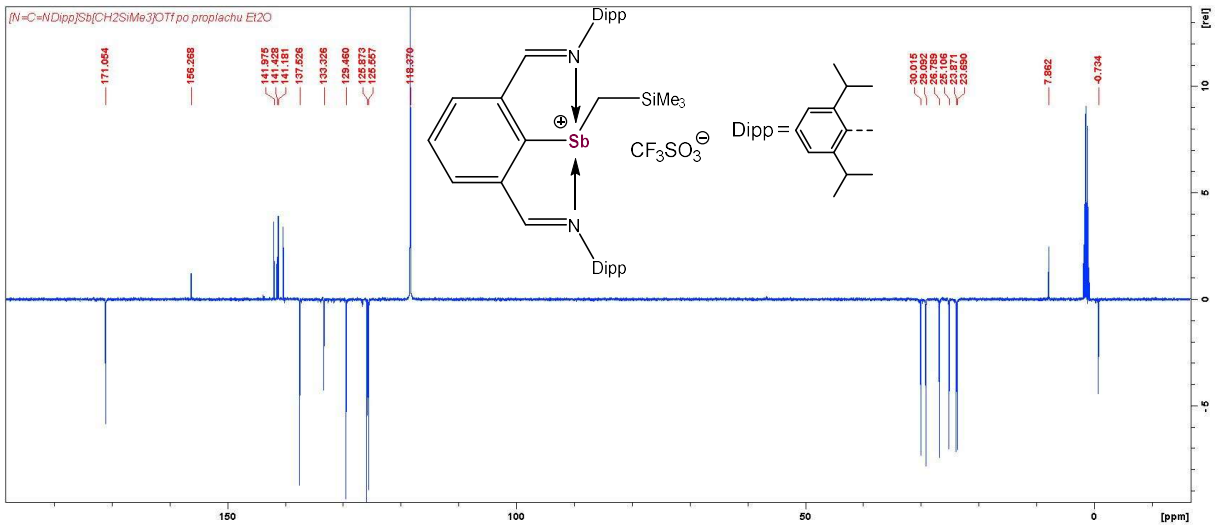

Figure S2: $^{13}C\{^{1}H\}$-APT NMR spectrum of **2-Sb** in CD_3CN (125.6 MHz).

Synthesis of 2-Bi

826 mg (1.25 mmol) of **1-Bi** was dissolved in benzene (15 mL) and 250 µL (1.25 mmol) of neat Me_3SiCH_2OTf was added. The solution was stirred for 12 h at r.t. and the reaction mixture was evaporated. The solid residue was washed with hexane (*ca* 2x10 mL) and dried *in vacuo* giving **2-Bi** as a white powder. The product can re-crystallized from dichloromethane/hexane mixture. Yield 800 mg, 71%, m.p. 190-192 °C. Anal. Calcd for $C_{37}H_{50}BiF_3N_2O_3SSi$ (Mr = 896.94): C, 49.6 %; H, 5.6 %; N, 3.1 %. Found: C, 49.5 %; H 5.7 %; N, 3.3 %. ^{1}H NMR (500 MHz, CD_3CN): δ -0.37 [9H, s, $Si(CH_3)_3$]; 1.11 [6H, d, $^{3}J_{H,H}$ = 6.7 Hz, *i*Pr-CH_3]; 1.19 [6H, d, $^{3}J_{H,H}$ = 6.7 Hz, *i*Pr-CH_3]; 1.24 [2H, s, $SiCH_2$]; 1.27 [12H, m, *i*Pr-CH_3]; 2.72 [2H, h, $^{3}J_{H,H}$ = 6.8 Hz, *i*Pr-CH]; 3.01 [2H, h, $^{3}J_{H,H}$ = 6.7 Hz, *i*Pr-CH]; 7.31-7.36 [6H, m, Ar-*H*]; 8.13 [1H, t, $^{3}J_{H,H}$ = 7.7 Hz, Ar-*H*]; 8.57 [2H, d, $^{3}J_{H,H}$ = 7.7 Hz, Ar-*H*]; 9.68 [2H, s, CH=N] ppm. $^{13}C\{^{1}H\}$ NMR (125.76 MHz, CD_3CN): δ 0.6 [$Si(CH_3)_3$]; 23.3 [*i*Pr-CH_3]; 24.3 [*i*Pr-CH_3]; 24.9 [*i*Pr-CH_3]; 26.6 [*i*Pr-CH_3]; 29.0 [*i*Pr-CH]; 30.1 [*i*Pr-CH]; 34.2 [$SiCH_2$]; 122.2 [t, $^{1}J_{F,C}$ = 325 Hz, CF_3], 125.2 [Ar-*C*]; 125.8 [Ar-*C*]; 129.0 [Ar-*C*]; 131.9 [Ar-*C*]; 139.6 [Ar-*C*]; 140.3 [Ar-*C*]; 141.6 [Ar-*C*]; 143.5 [Ar-*C*]; 147.4 [Ar-*C*]; 176.0 [CH=N]; 192.0 [*C*-ipso] ppm.

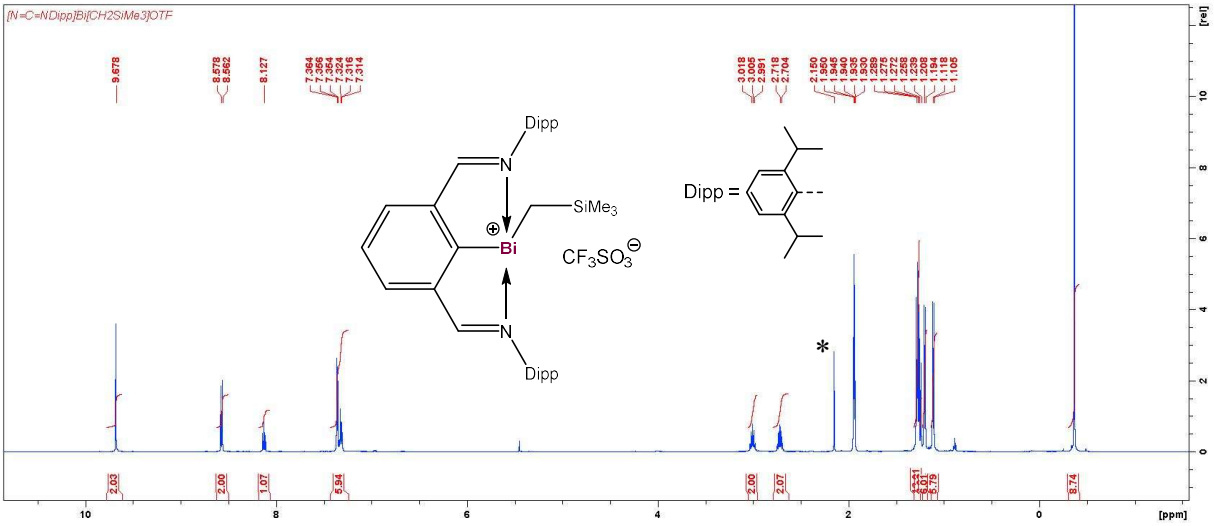

Figure S3: ^{1}H NMR spectrum of **2-Bi** in CD_3CN (500 MHz). *denotes traces of moisture in CD_3CN.

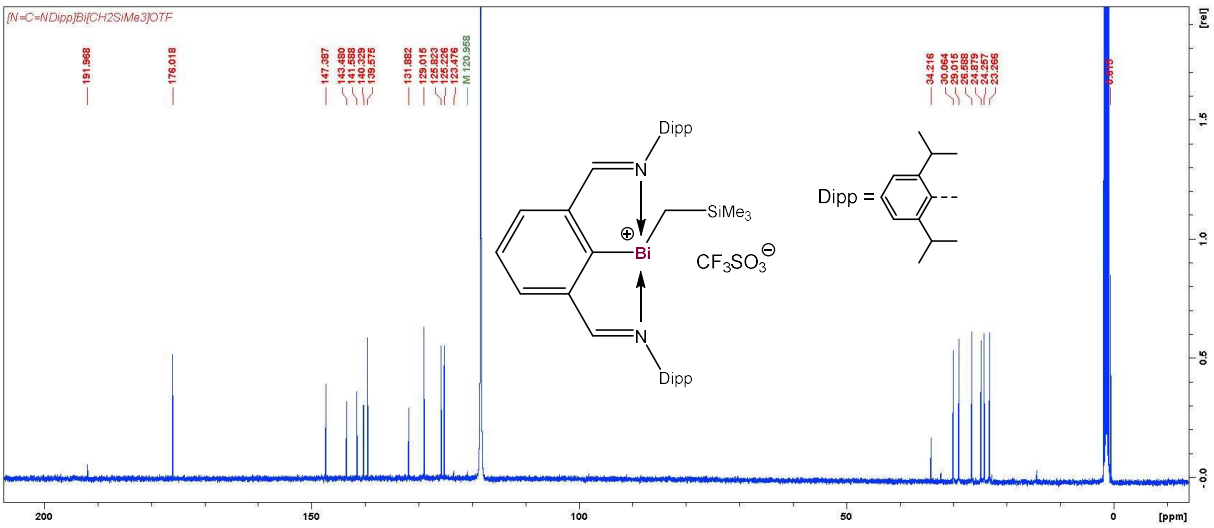

Figure S4: $^{13}C\{^{1}H\}$ NMR spectrum of **2-Bi** in CD_3CN (125.6 MHz).

Synthesis of 4-Sb

1.002 g (2.61 mmol) of **3-Sb** was dissolved in thf (40 mL), cooled to -25 °C and 5.22 mL (5.22 mmol) of 1M solution of $K[BEt_3H]$ in thf as added dropwise. The yellow solution was stirred for 10 min at -25 °C and for additional 30 min at r.t. Subsequently, 0.52 mL (2.61 mmol) of neat Me_3SiCH_2OTf was added. The solution was stirred for 1 h at r.t. and the reaction mixture was evaporated. The solid residue was washed with hexane (*ca* 2x10 mL) and dried *in vacuo*. Thus, obtained solid was extracted with acetonitrile (50 mL) and the clear colorless extract was

evaporated to give **4-Sb** as a white powder. The product can re-crystallized from thf/hexane mixture. Yield 592 mg, 42%, m.p. 132-137 °C. Anal. Calcd for $C_{17}H_{30}F_3N_2O_3SSbSi$ (Mr = 549.34): C, 37.2 %; H, 5.5 %; N, 5.1 %. Found: C, 37.6 %; H 5.7 %; N, 5.3 %. ^{1}H NMR (400 MHz, CD_3CN): δ 0.22 [9H, s, Si(CH_3)$_3$]; 0.87 [2H, s, SiCH_2]; 2.57 [6H, s, N(CH_3)$_2$]; 2.64 [6H, s, N(CH_3)$_2$]; 3.91 and 3.99 [4H, AB pattern, $^2J_{H,H}$ = 15.1 Hz, NCH_2]; 7.27 [2H, d, $^3J_{H,H}$ = 7.5 Hz, Ar-*H*]; 7.44 [1H, t, $^3J_{H,H}$ = 7.5 Hz, Ar-*H*] ppm. ^{13}C{^{1}H} NMR (100.6 MHz, CD_3CN): δ 1.1 [Si(*C*H$_3$)$_3$]; 8.6 [Si*C*H$_2$]; 47.2 [N(*C*H$_3$)$_2$]; 48.2 [N(CH_3)$_2$]; 65.4 [N*C*H$_2$]; 122.1 [t, $^1J_{F,C}$ = 322 Hz, *C*F$_3$], 126.6 [Ar-*C*]; 131.9 [Ar-*C*]; 142.9 [*C*-ipso]; 144.6 [Ar-*C*] ppm.

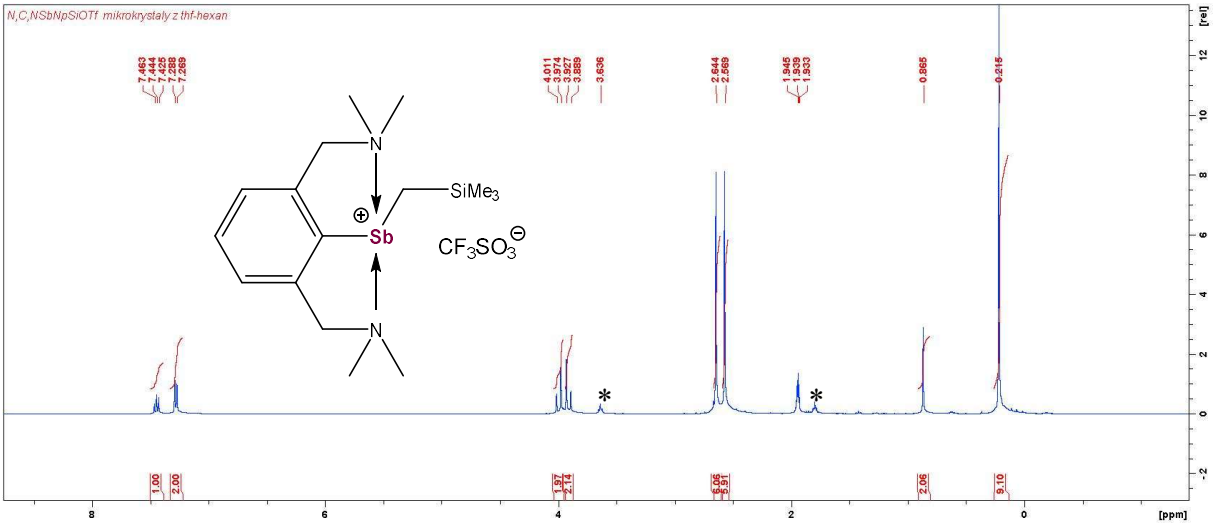

Figure S5: ^{1}H NMR spectrum of **4-Sb** in CD_3CN (400 MHz). *denotes traces of thf.

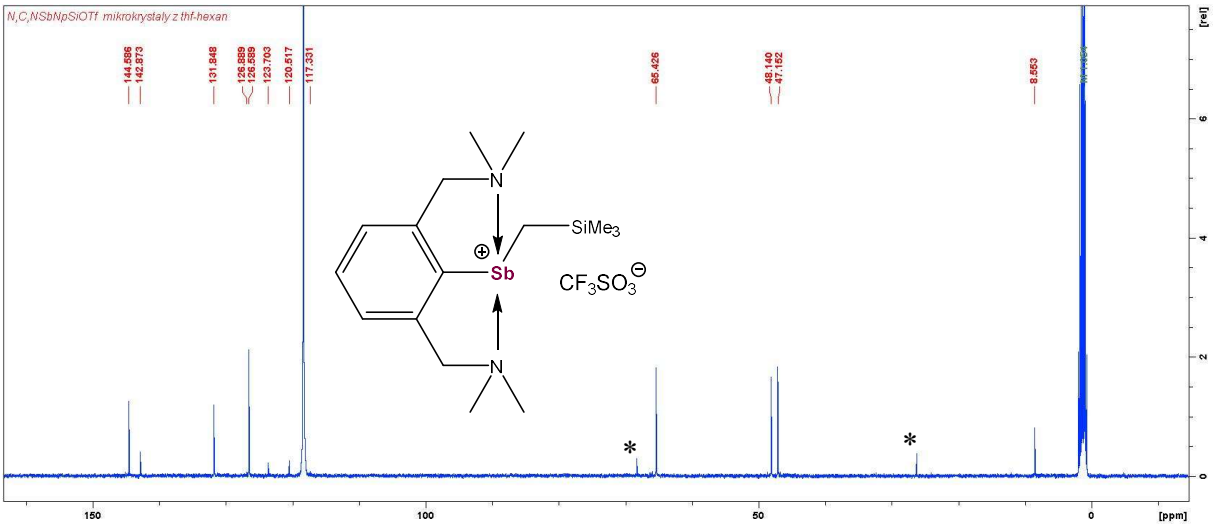

Figure S6: $^{13}C\{^{1}H\}$ NMR spectrum of **4-Sb** in CD_3CN (125.6 MHz). *denotes traces of thf.

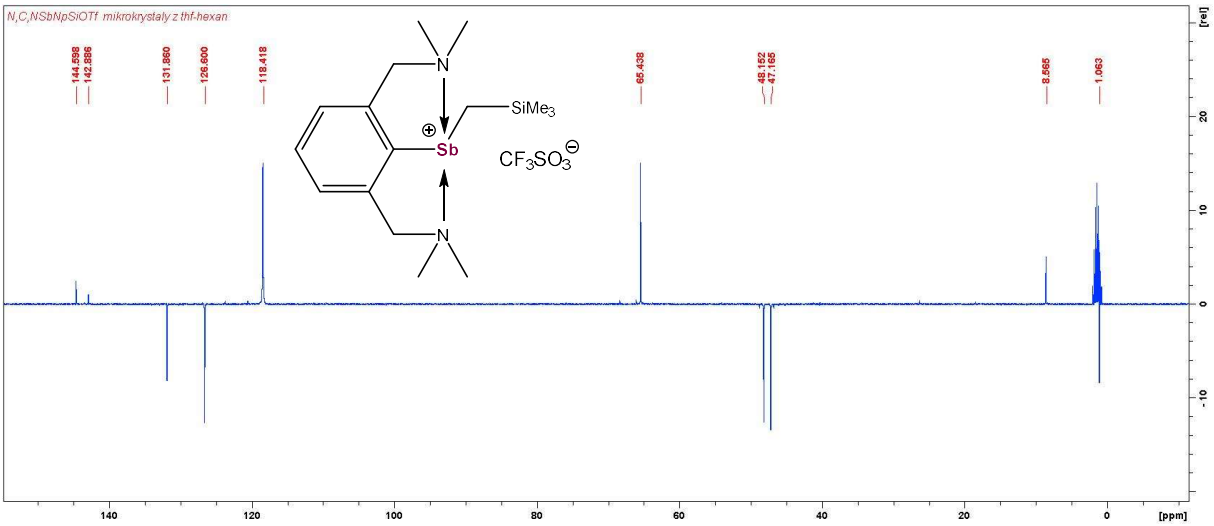

Figure S7: $^{13}C\{^{1}H\}$-APT NMR spectrum of **4-Sb** in CD_3CN (125.6 MHz).

Synthesis of 5-Sb

2.189 g (5.7 mmol) of **3-Sb** was mixed with thf (60 mL), cooled to -25 °C and 11.4 mL (11.4 mmol) of 1M solution of $K[BEt_3H]$ in thf as added dropwise. The orange solution was stirred for 10 min at -25 °C and for additional 30 min at r.t. Subsequently, 0.36 mL (5.7 mmol) of neat MeI was added. The solution was stirred for 1 h at r.t. and the reaction mixture was evaporated. The solid residue was washed with hexane (*ca* 2x10 mL) and dried *in vacuo*. Thus, obtained solid was extracted with acetonitrile (30 mL) and the clear colorless extract was evaporated and washed with hexane (10 mL) give **5-Sb** as a white powder. Yield 1.532 g, 59%, m.p. 227-230 °C. Anal. Calcd for $C_{13}H_{22}IN_2Sb$ (Mr = 455.00): C, 34.3 %; H, 4.9 %; N, 6.2 %. Found: C, 34.8 %; H 5.2 %; N, 6.3 %. ^{1}H NMR (500 MHz, CD_3CN): δ 1.25 [3H, s, C*H*$_3$]; 2.57 [6H, s, N(C*H*$_3$)$_2$]; 2.69 [6H, s, N(C*H*$_3$)$_2$]; 3.94 and 3.99 [4H, AB pattern, $^{2}J_{H,H}$ = 14.9 Hz, NC*H*$_2$]; 7.28 [2H, d, $^{3}J_{H,H}$ = 7.5 Hz, Ar-*H*]; 7.43 [1H, t, $^{3}J_{H,H}$ = 7.5 Hz, Ar-*H*] ppm. $^{13}C\{^{1}H\}$ NMR (100.6 MHz, CD_3CN): δ 6.7 [*C*H$_3$]; 46.7 [N(*C*H$_3$)$_2$]; 48.1 [N(C*H*$_3$)$_2$]; 65.8 [N*C*H$_2$]; 126.3 [Ar-*C*]; 131.5 [Ar-*C*]; 143.2 [*C*-ipso]; 144.5 [Ar-*C*] ppm.

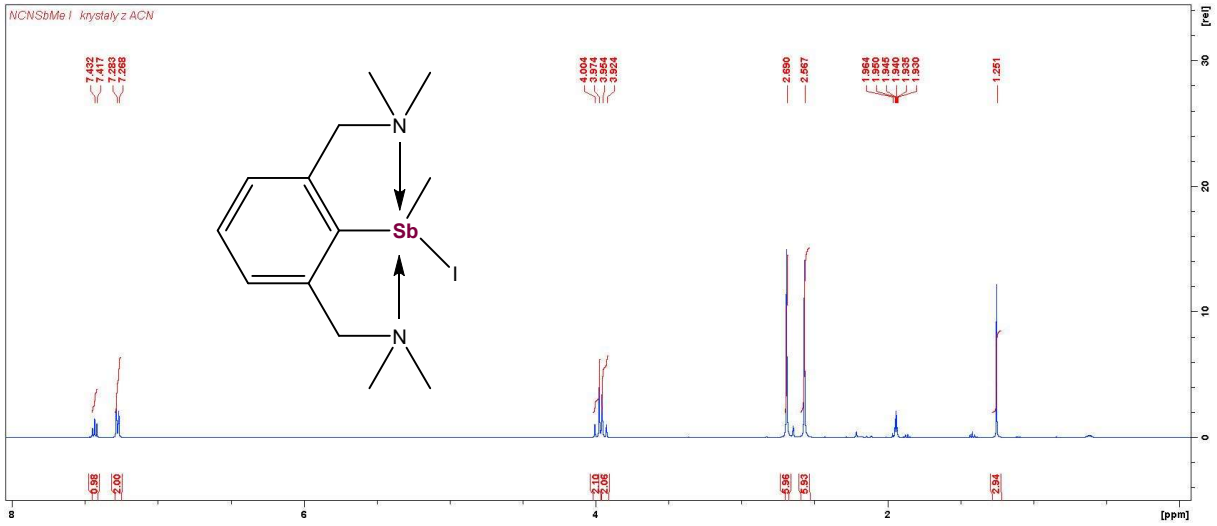

Figure S8: ^{1}H NMR spectrum of **5-Sb** in CD_3CN (500 MHz).

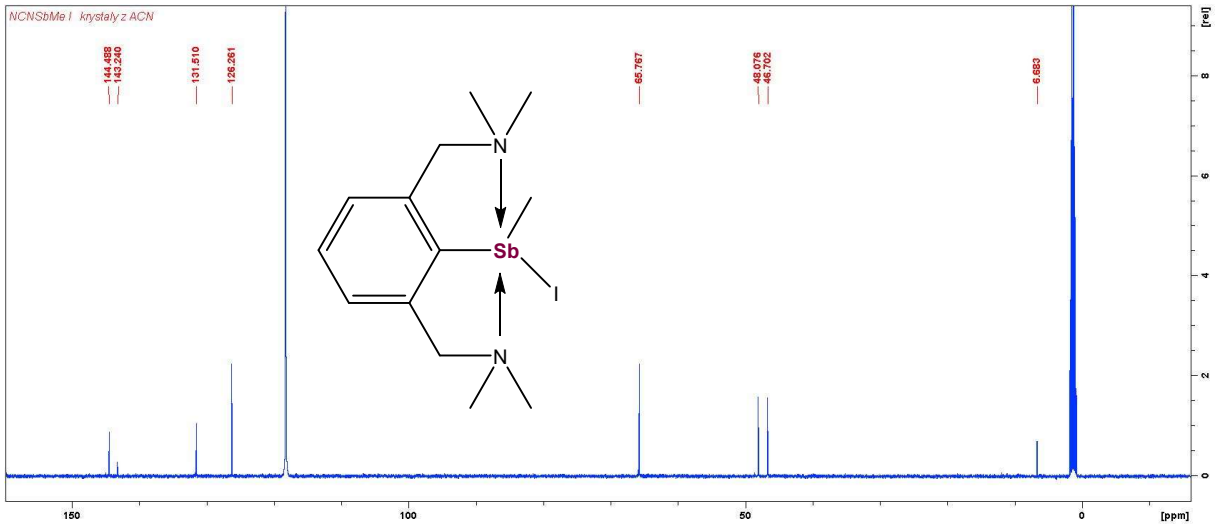

Figure S9: $^{13}C\{^{1}H\}$ NMR spectrum of **5-Sb** in CD_3CN (125.6 MHz).

2) NMR spectra of studied compounds.

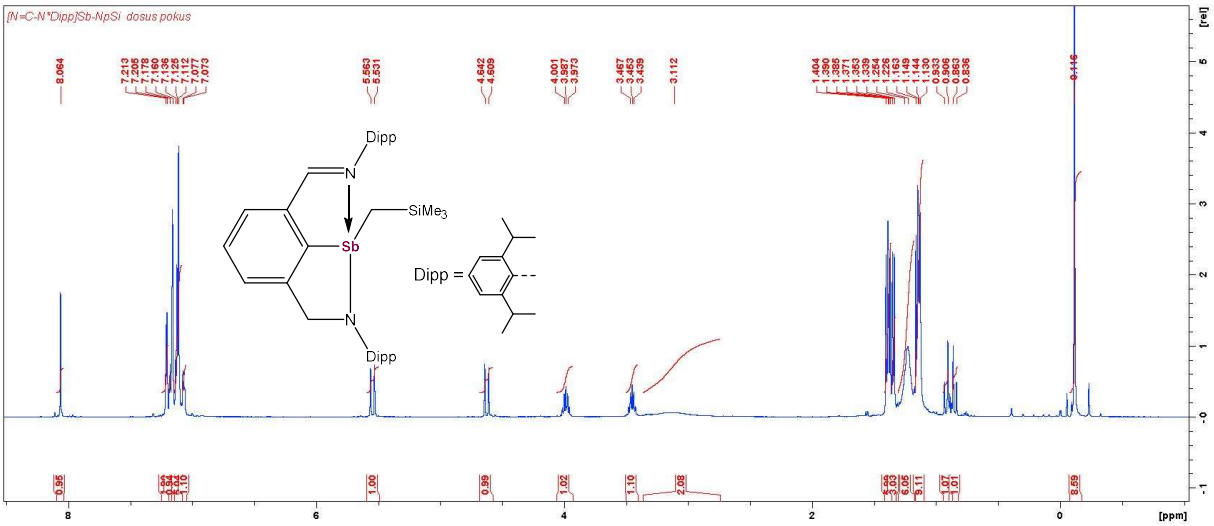

Figure S10: ^{1}H NMR spectrum of **6-Sb** in C_6D_6 (500 MHz).

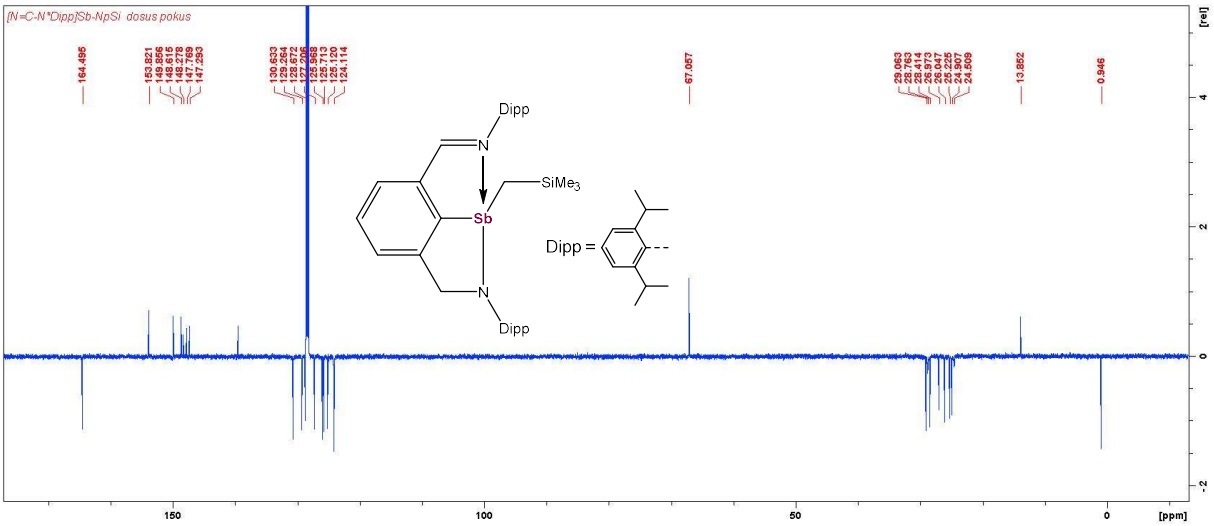

Figure S11: $^{13}C\{^{1}H\}$-APT NMR spectrum of **6-Sb** in C_6D_6 (125.6 MHz).

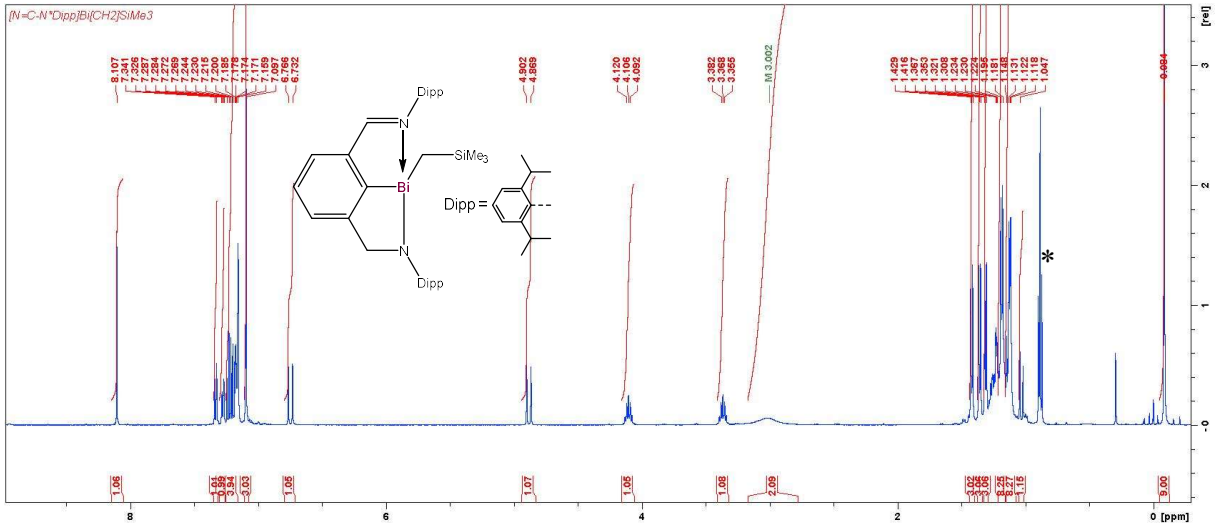

Figure S12: ^{1}H NMR spectrum of **6-Bi** in C_6D_6 (500 MHz). *denotes traces of hexane present in dissolved single-crystals.

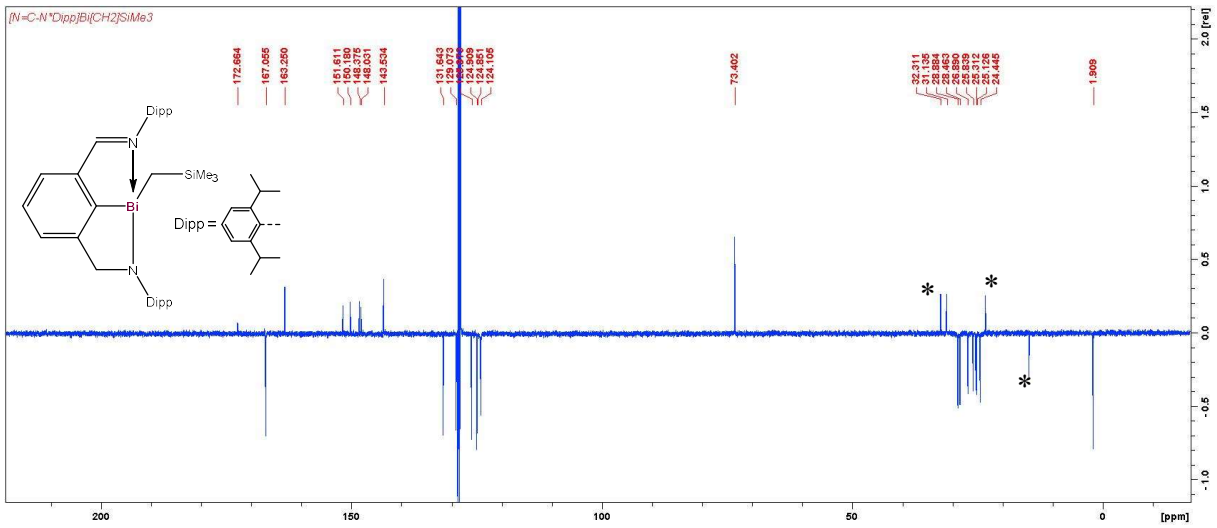

Figure S13: ^{13}C{^{1}H}-APT NMR spectrum of **6-Bi** in C_6D_6 (125.6 MHz). *denotes traces of hexane present in dissolved single-crystals.

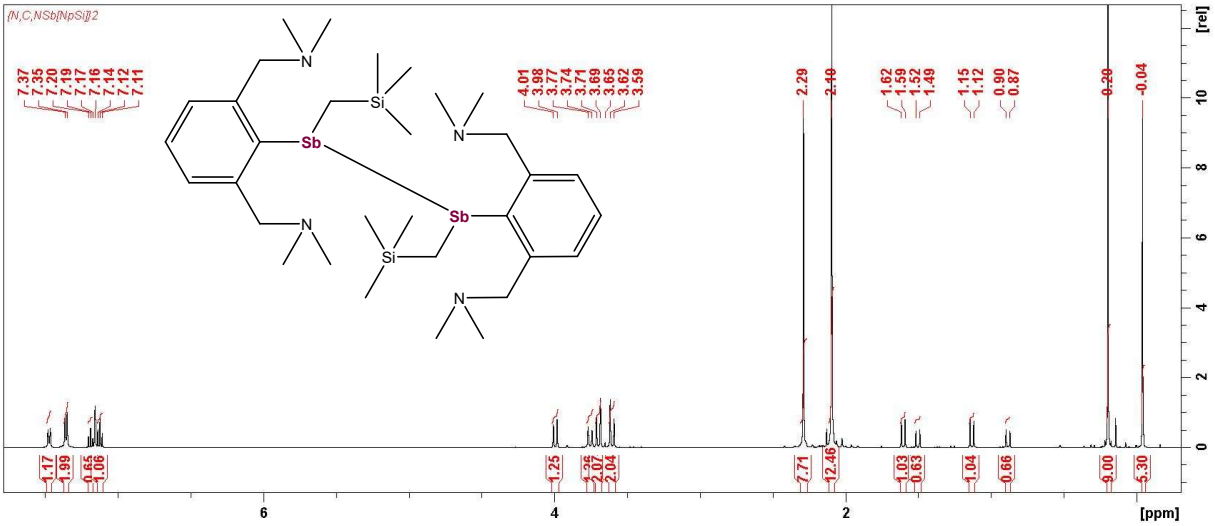

Figure S14: ^{1}H NMR spectrum of *meso*-**7-Sb** and *rac*-*RR*/*SS*-**7-Sb** in C_6D_6 (500 MHz).

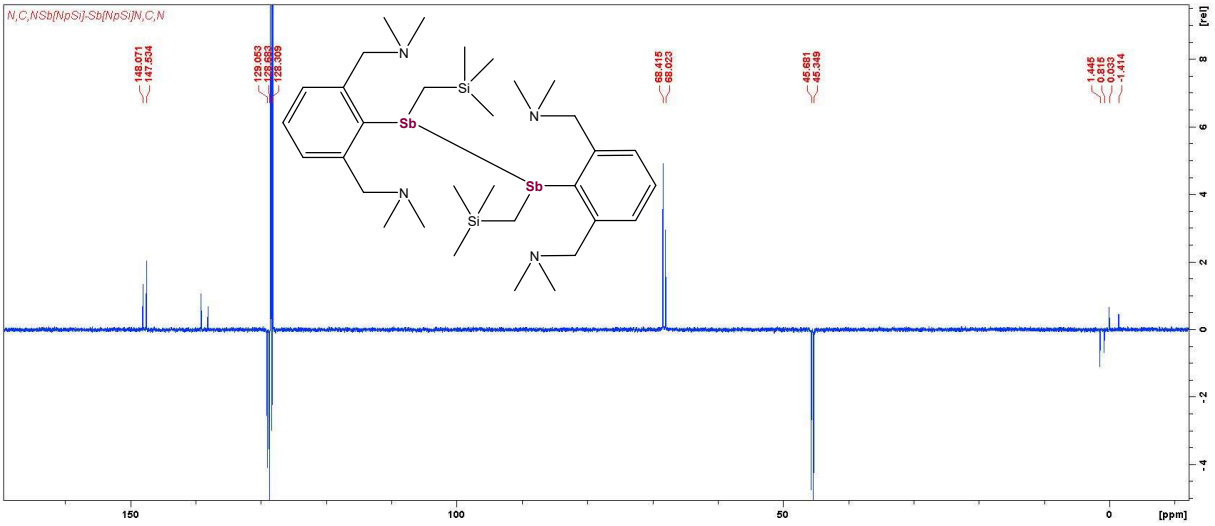

Figure S15: ^{13}C{^{1}H}-APT NMR spectrum of *meso*-**7-Sb** and *rac*-*RR*/*SS*-**7-Sb** in C_6D_6 (125.6 MHz).

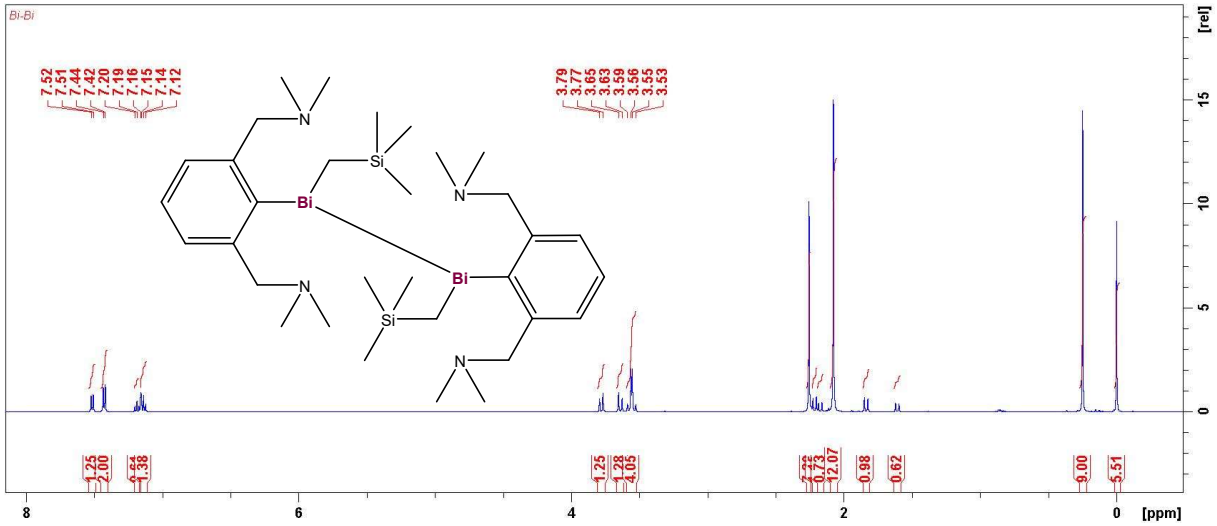

Figure S16: ^{1}H NMR spectrum of *meso*-**7-Bi** and *rac*-*RR*/*SS*-**7-Bi** in C_6D_6 (400 MHz).

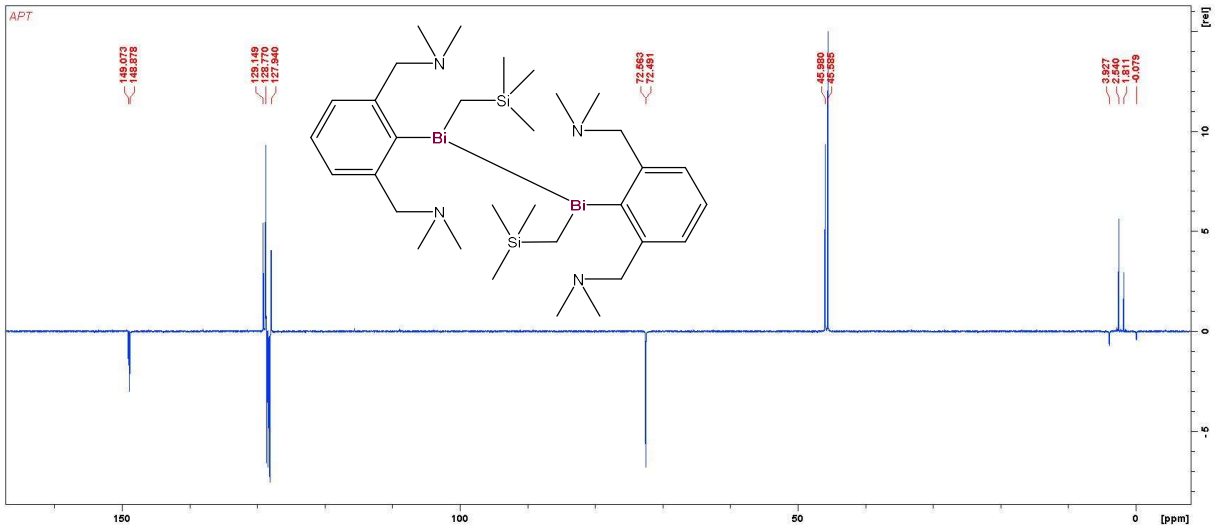

Figure S17: $^{13}C\{^{1}H\}$-APT NMR spectrum of *meso*-**7-Bi** and *rac*-*RR*/*SS*-**7-Bi** in C_6D_6 (100.2 MHz).

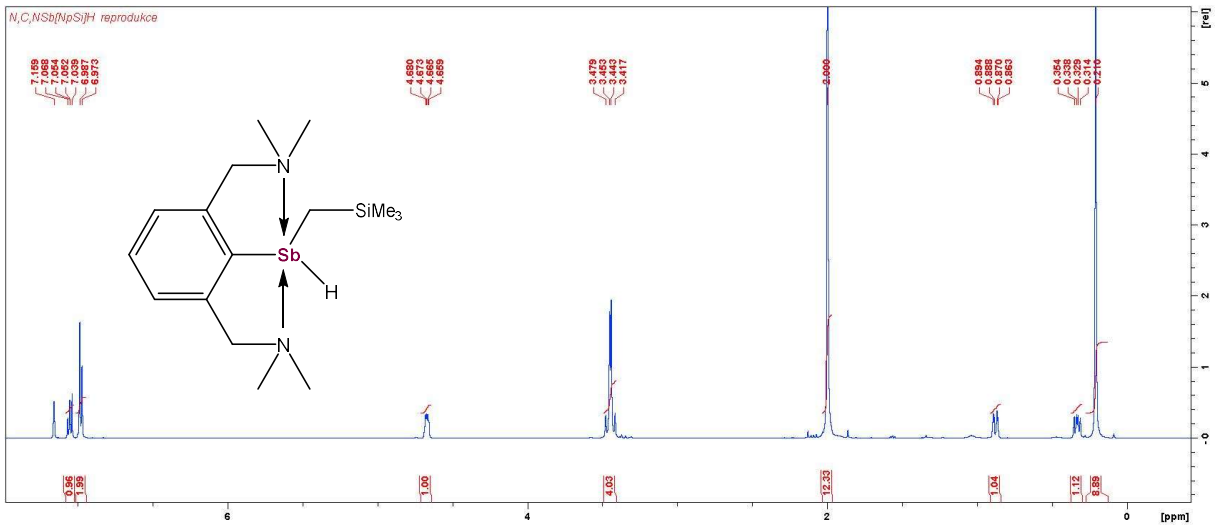

Figure S18: ^{1}H NMR spectrum of **9-Sb** in C_6D_6 (500 MHz).

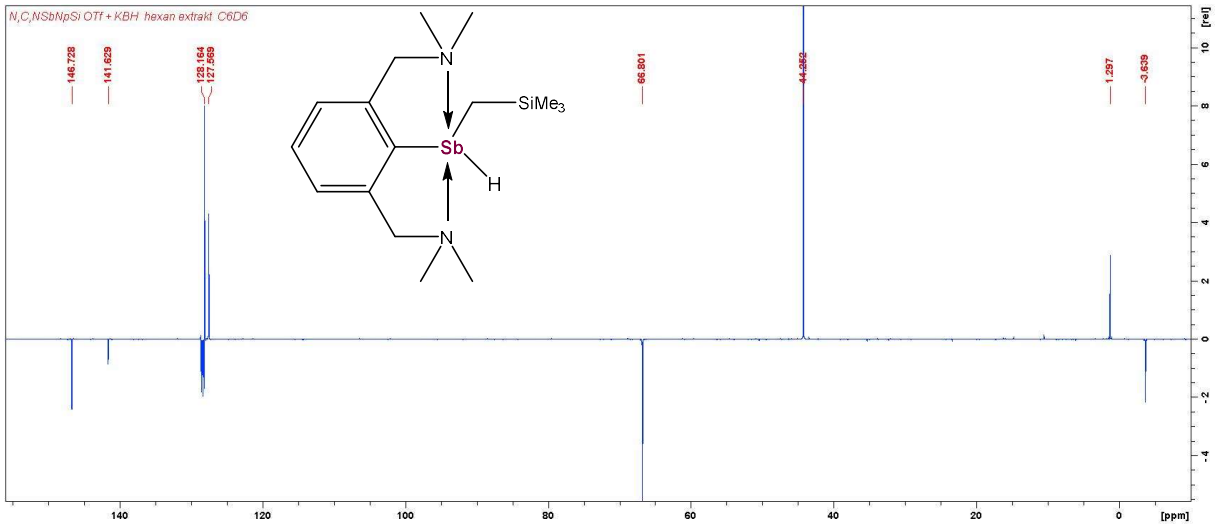

Figure S19: ^{13}C{^{1}H}-APT NMR spectrum of **9-Sb** in C_6D_6 (125.6 MHz).

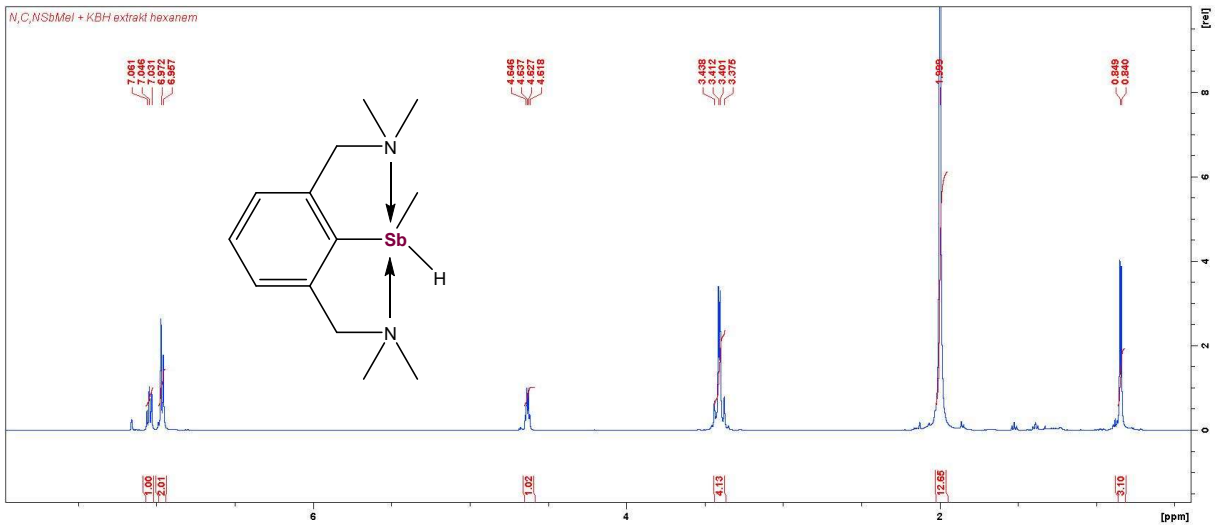

Figure S20: ^{1}H NMR spectrum of **10-Sb** in C_6D_6 (500 MHz).

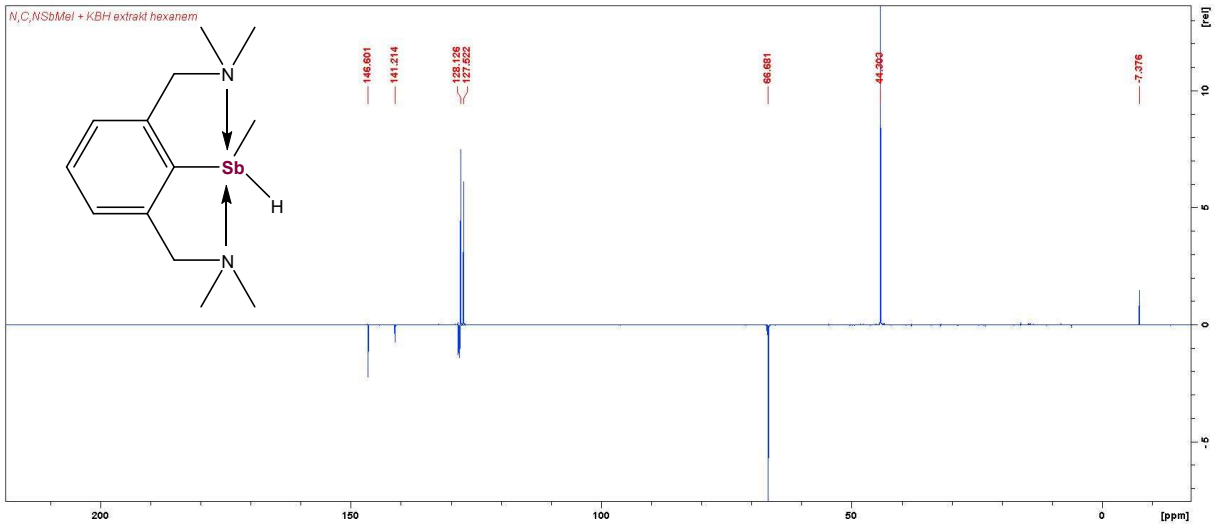

Figure S21: ^{13}C{^{1}H}-APT NMR spectrum of **10-Sb** in C_6D_6 (125.6 MHz).

3) NMR spectra of important reaction mixtures.

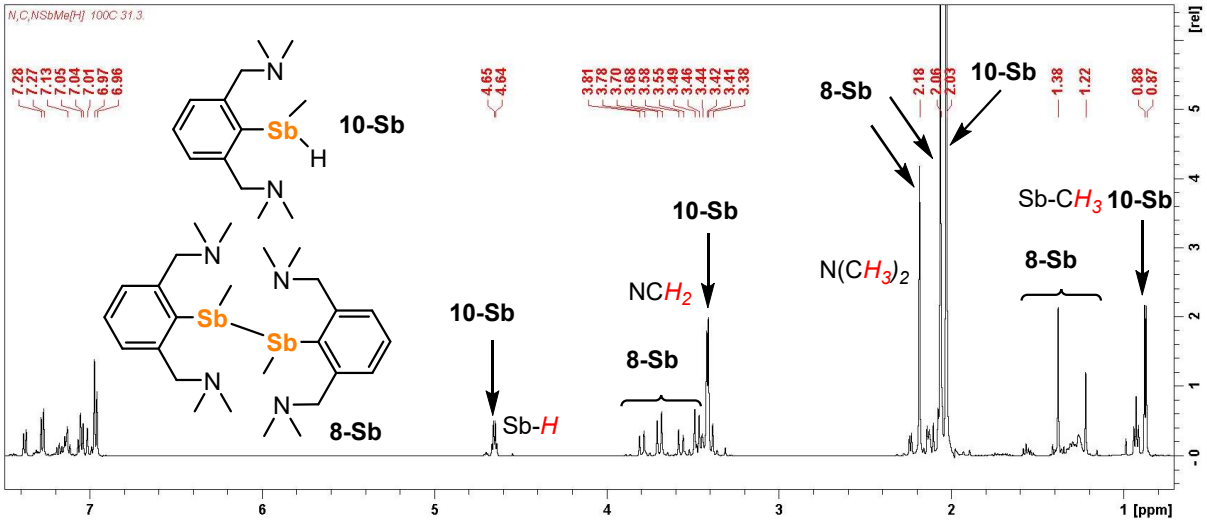

Figure S22: ^{1}H NMR spectra showing mixture after heating of **10-Sb** neat (90 °C, 5 days) resulting in partial formation of mixture *meso*-**8-Sb** and *rac-RR/SS*-**8-Sb** along with the starting material.

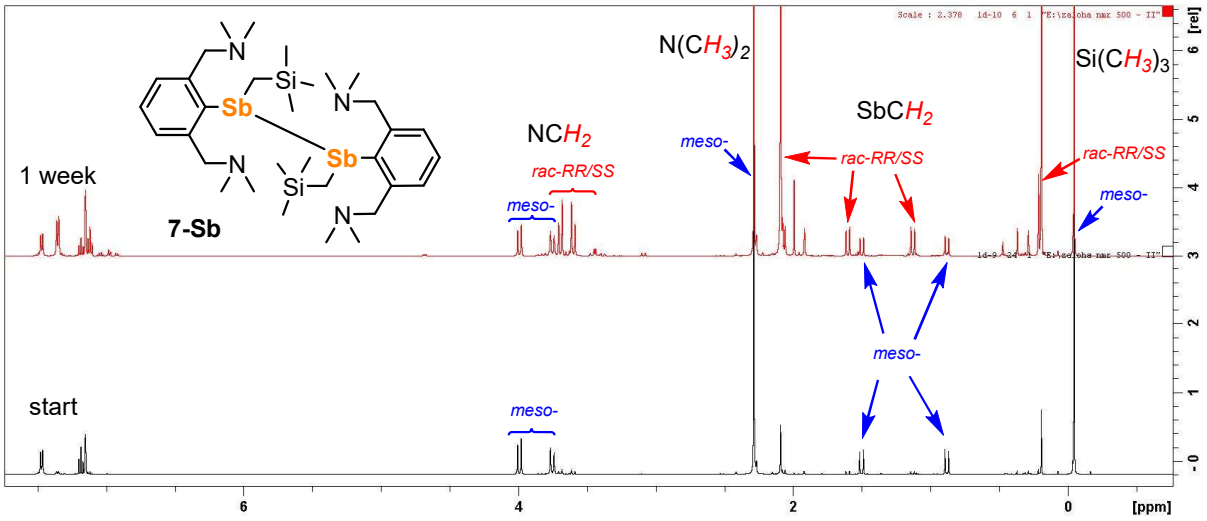

Figure S23: ^{1}H NMR spectra of *meso*-**7-Sb** (bottom) and formation of its mixture with *rac-RR/SS*-**7-Sb** (0.6:1, top). Bulk sample after crystallization dissolved and sealed in C_6D_6 (500 MHz).

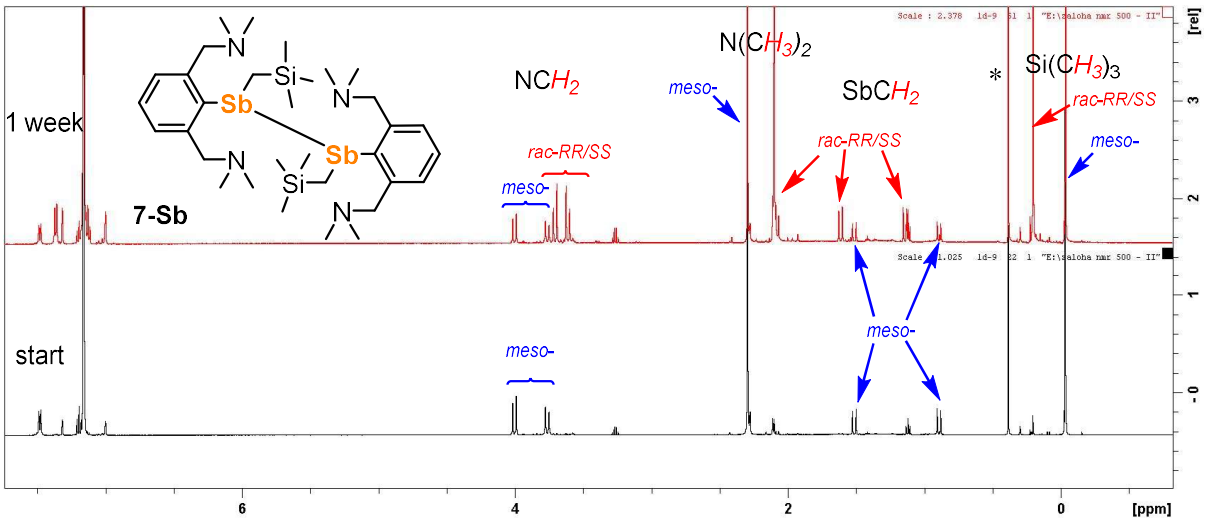

Figure S24: ^{1}H NMR spectra of *meso*-**7-Sb** (bottom) and formation of its mixture with *rac-RR/SS*-**7-Sb** (0.6:1, top). One single-crystal dissolved and sealed in C_6D_6 (ns = 50, 500 MHz). *denotes a trace amount of moisture visible due to the extremely low concentration of the sample.

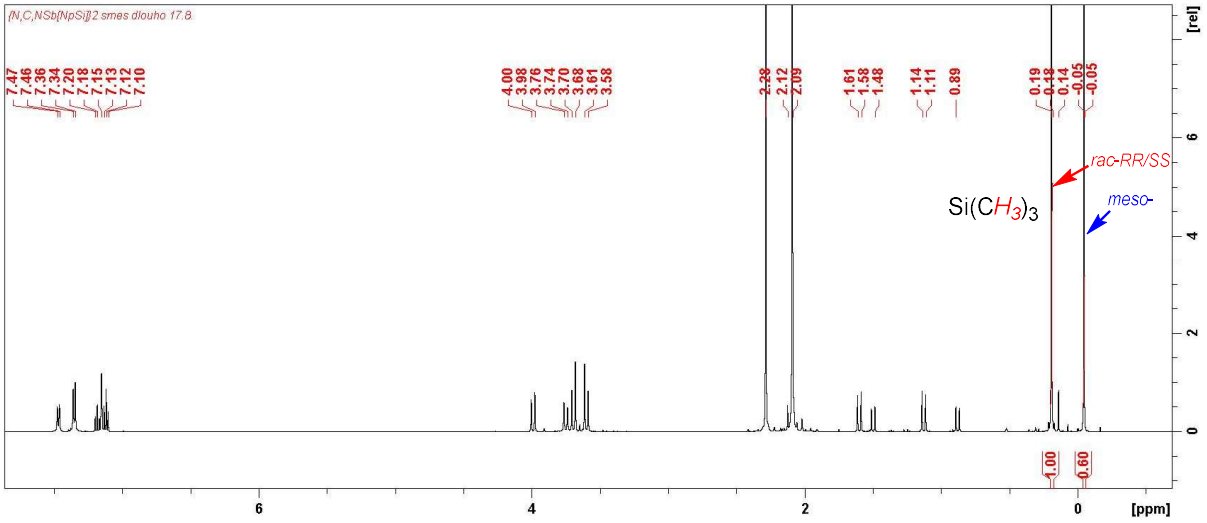

Figure S25: ^{1}H NMR spectra showing mixture of a bulk sample *meso*-**7-Sb** and *rac-RR/SS*-**7-Sb** (0.6:1) after two months sealed in C_6D_6 (500 MHz).

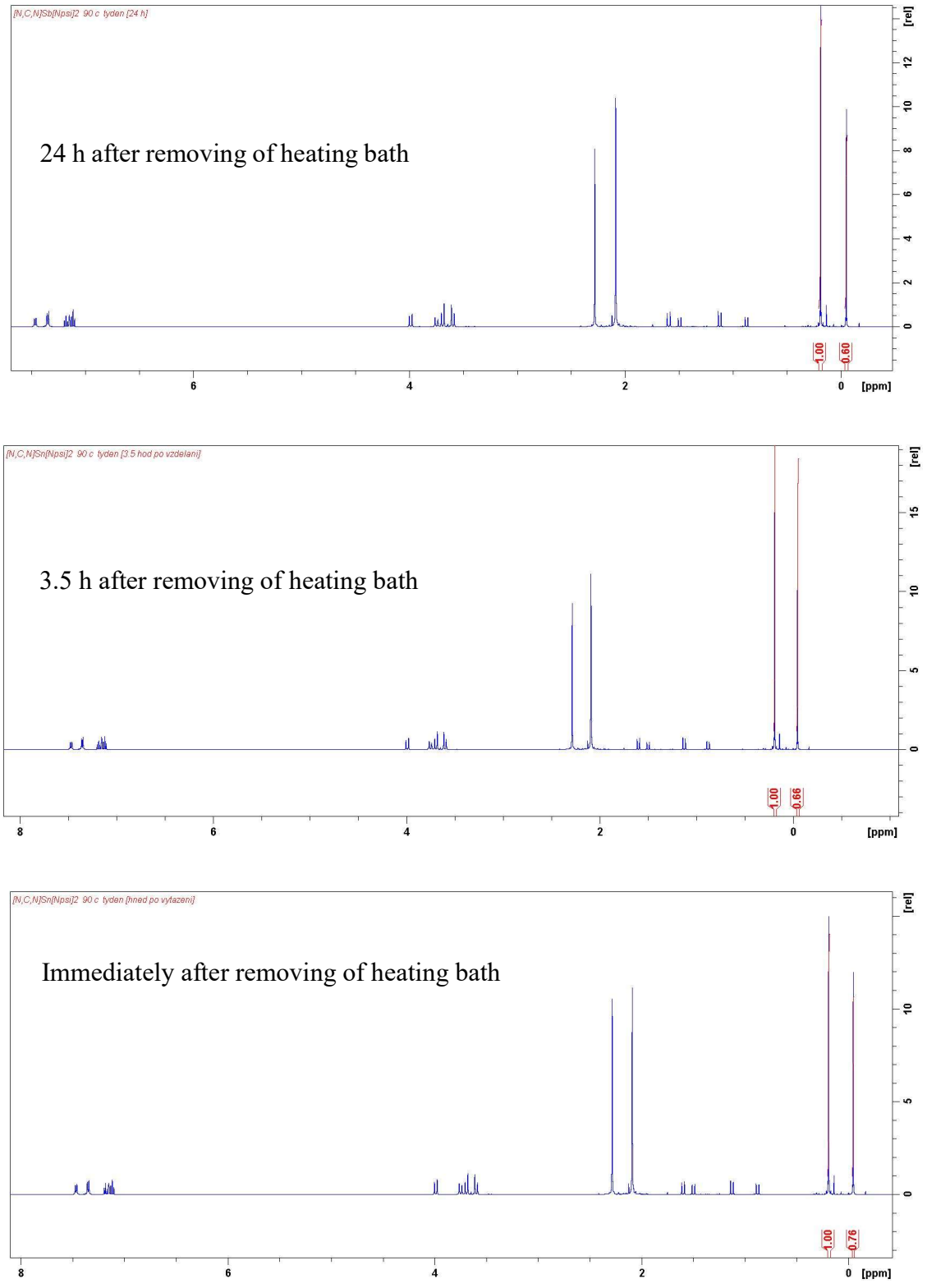

Figure S26: ^{1}H NMR spectra showing mixture of a bulk sample *meso*-**7-Sb** and *rac*-*RR*/*SS*-**7-Sb** after 1 week of heating (90 °C) sealed in C_6D_6 (ratio 0.76:1, bottom) and then leaving the sample at r.t. to recover the original mutual ratio of 0.6:1 (3.5 and 24h, top spectra) (500 MHz).

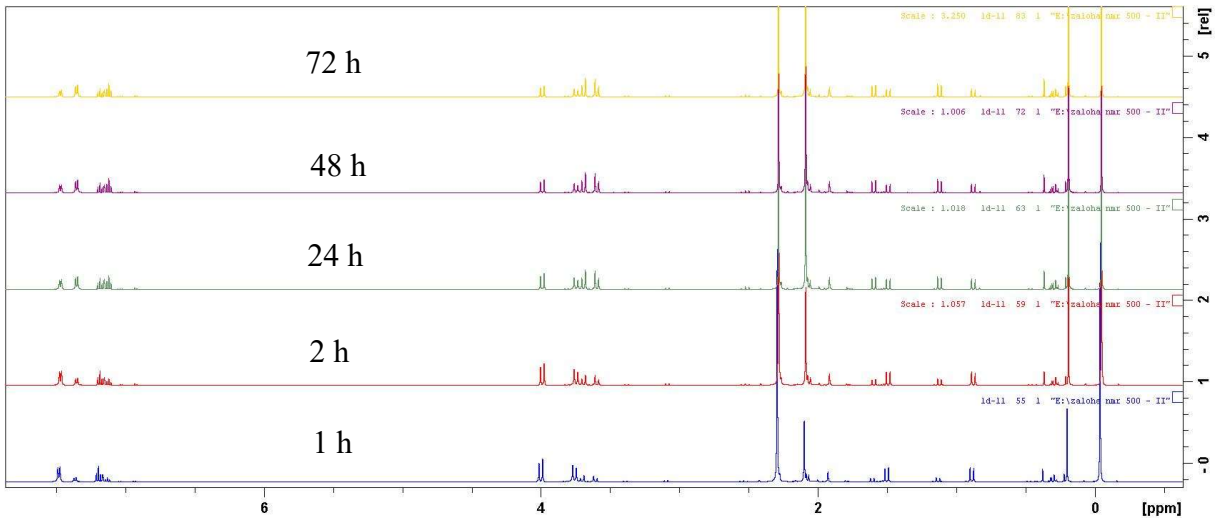

Figure S27: ^{1}H NMR spectra showing gradual conversion of *meso*-**7-Sb** to its mixture with *rac*-*RR*/*SS*-**7-Sb** at r.t. in C_6D_6 (the final ration again 0.6:1, 500 MHz).

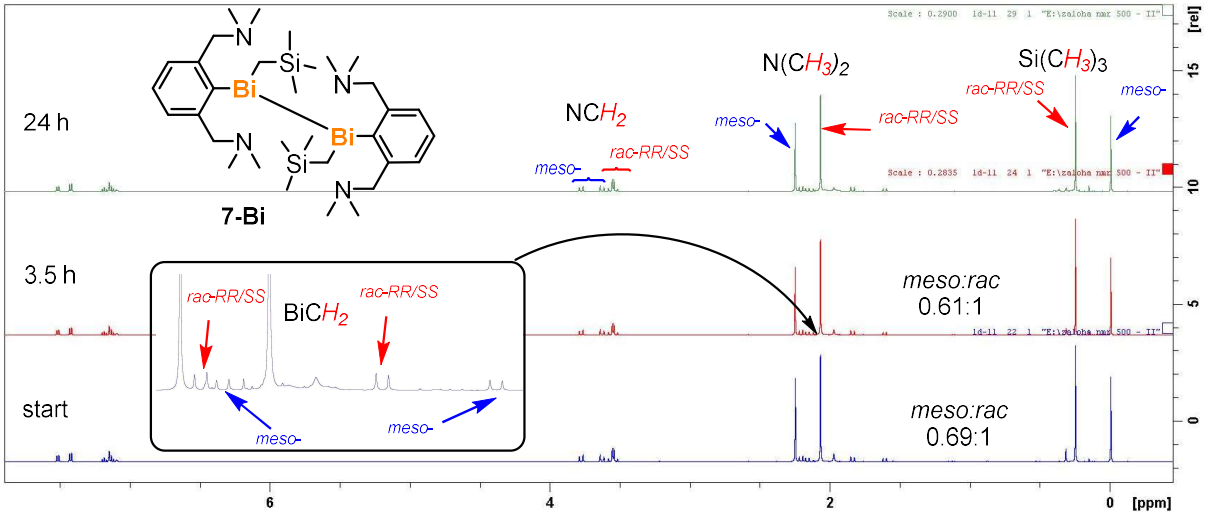

Figure S28: ^{1}H NMR spectra of mixture of *meso*-**7-Bi** and *rac*-*RR*/*SS*-**7-Bi** obtained upon dissolving bulk sample (ratio 0.69:1) after crystallization and sealed in C_6D_6 (bottom) and after 3.5 and 24 h (top, final ratio 0.61:1, 500 MHz).

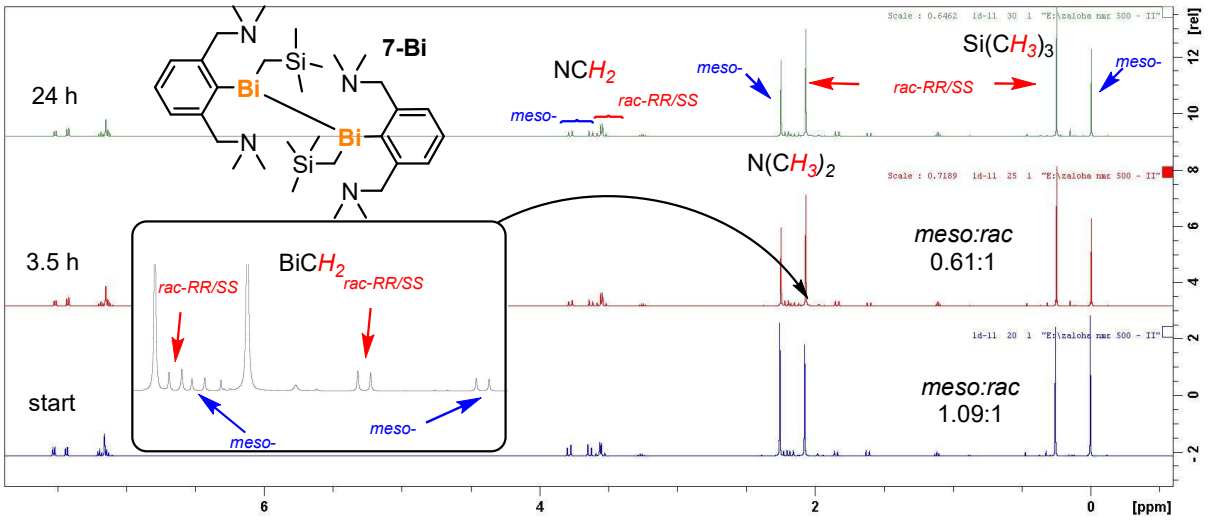

Figure S29: ^{1}H NMR spectra of mixture of *meso*-**7-Bi** and *rac-RR/SS*-**7-Bi** (ratio 1.09:1) obtained upon dissolving one single crystal of *meso*-**7-Bi** sealed in C_6D_6 (bottom) and after 3.5 and 24 h (top, final ratio 0.61:1, 500 MHz).

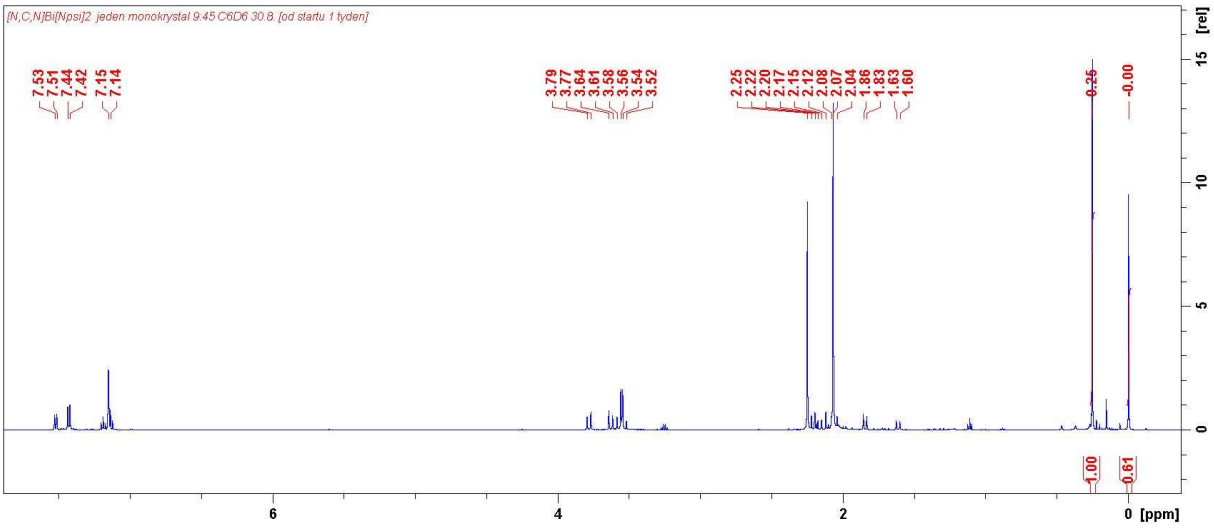

Figure S30: ^{1}H NMR spectrum of mixture of *meso*-**7-Bi** and *rac-RR/SS*-**7-Bi** (ratio 0.61:1) after one week at r.t. (C_6D_6, 500 MHz).

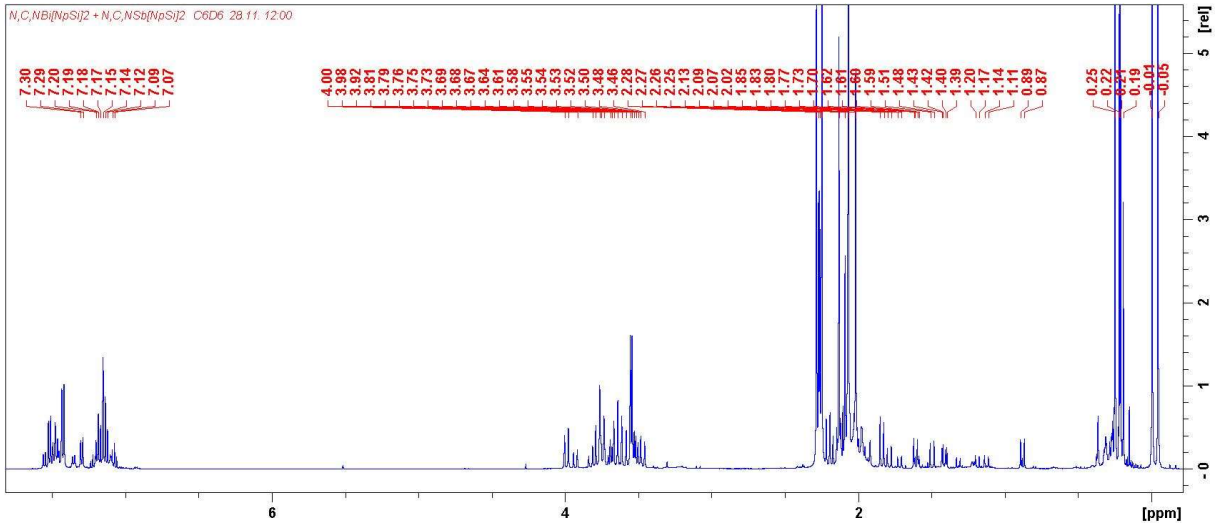

Figure S31: ^{1}H NMR spectrum of mixture of *meso/rac*-**7-Sb** and *meso*/*rac*-*RR*/*SS*-**7-Bi** after 72 h at r.t. (C_6D_6, 500 MHz).

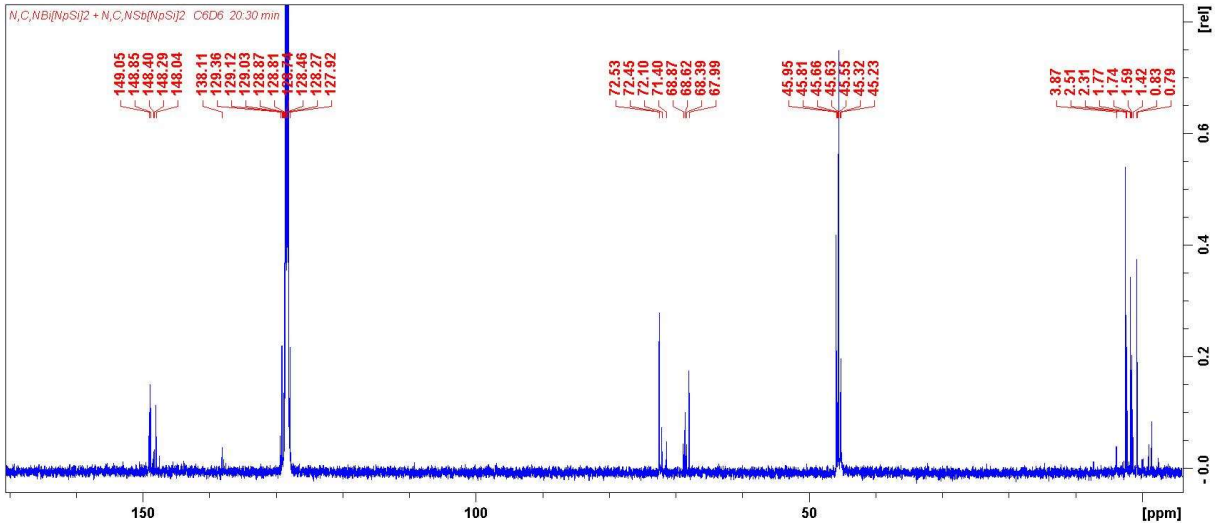

Figure S32: $^{13}C\{^{1}H\}$ NMR spectrum of mixture of *meso/rac*-**7-Sb** and *meso*/*rac*-*RR*/*SS*-**7-Bi** after 72 h at r.t. (C_6D_6, 500 MHz).

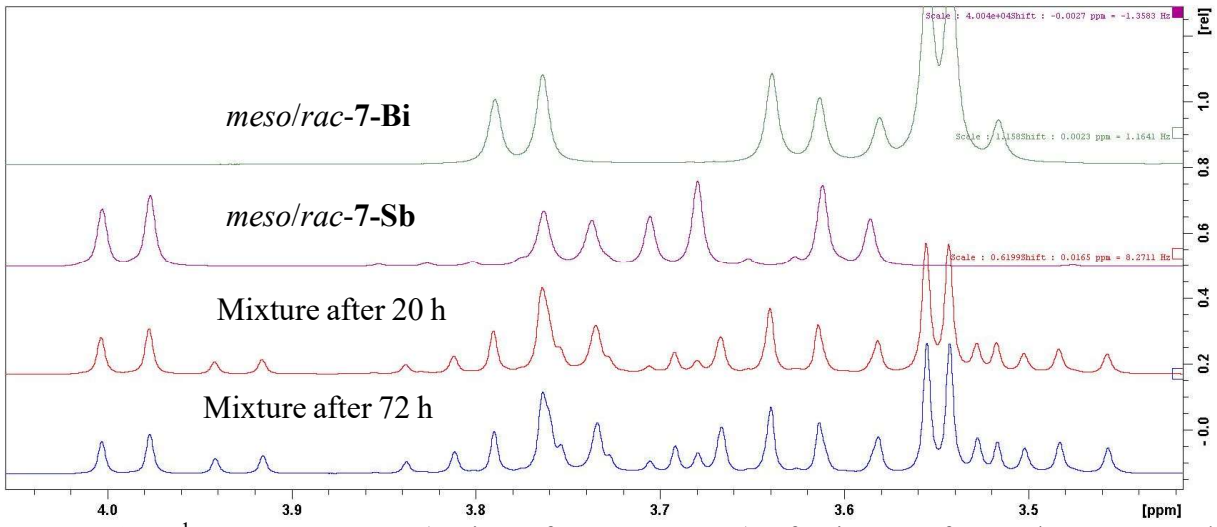

Figure S31: ^{1}H NMR spectra (region of CH_2N groups) of mixture of *meso/rac*-**7-Sb** and *meso*/*rac*-**7-Bi** after 72 h at r.t. along with pure samples of *meso/rac*-**7-Sb** and *meso*/*rac-RR*/*SS*-**7-Bi** for comparison (C_6D_6, 500 MHz).

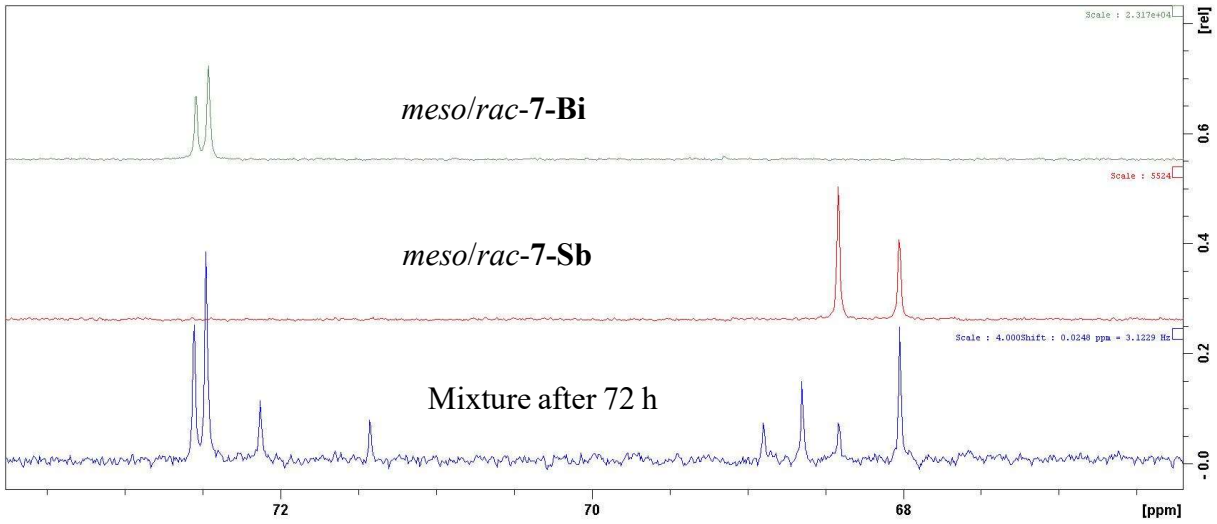

Figure S32: $^{13}C\{^{1}H\}$ NMR spectra (region of CH_2N groups) of mixture of *meso/rac*-**7-Sb** and *meso*/*rac*-**7-Bi** after 72 h at r.t. along with pure samples of *meso/rac*-**7-Sb** and *meso*/*rac-RR*/*SS*-**7-Bi** for comparison (C_6D_6, 500 MHz).

4) Crystallographic data for studied compounds.

Table S1. Crystal data and structure refinement of studied compounds.

	2-Bi	**4-Sb**	**6-Sb**
Formula	$C_{37}H_{50}BiF_3N_2O_3SSi$	$C_{17}H_{30}F_3N_2O_3SSbSi$	$C_{42}H_{65}N_2SbSi$
Formula weight, g mol^{-1}	896.92	549.33	747.80
Crystal system	Monoclinic	Triclinic	Orthorhombic
Crystal size, mm	0.59 × 0.27 × 0.15	0.40 × 0.07 × 0.05	0.59 × 0.53 × 0.37
Space group	P-2_1/n	P-1	P$na2_1$
a, Å	13.8907(7)	9.1611(7)	13.5556(5)
b, Å	13.5122(5)	10.0853(8)	18.2010(6)
c, Å	21.3741(9)	13.3015(10)	16.9952(6)
α, º	90	87.219(3)	90
β, º	92.234(2)	79.274(3)	90
γ, º	90	72.520(3)	90
V, Å^3	4008.7(3)	1151.69(16)	4193.1(3)
Z	4	2	4
ρ_{calcd}, Mg m^{-3}	1.4863	1.584	1.185
μ (Mo *K*α), mm^{-1}	4.529	1.384	0.715
F(000)	1800	556	1584
θ range, deg	1 to 26.5	1 to 30.0	1 to 29.0
No. of reflns collected	85620	42574	32788
No. indep. Reflns	8304	7535	7888
No. obsd reflns with ($I>2\sigma(I)$), R_{int}	6387, 0.058	5697, 0.072	6376, 0.036
No. refined params	453	288	439
GooF (F^2)	1.053	1.108	1.027
R_1 (F) ($I > 2\sigma(I)$)	0.044	0.053	0.039
wR_2 (F^2) (all data)	0.063	0.093	0.085
Largest diff peak/hole, e Å^{-3}	1.095 / –1.446	2.175 / –1.325	0.598 / –0.369
CCDC	2203728	2203729	2203732

$R_{int} = \sum |F_o^2 - F_{o,mean}^2| / \sum F_o^2$, $S = [\sum(w(F_o^2 - F_c^2)^2)/(N_{diffrs} - N_{params})]^{½}$ for all data, $R(F) = \sum ||F_o| - |F_c|| / \sum |F_o|$ for observed data, $wR(F^2) = [\sum(w(F_o^2 - F_c^2)^2)/(\sum w(F_o^2)^2)]^{½}$ for all data.

Table S1 (continuation). Crystal data and structure refinement of studied compounds.

	6-Bi	**7-Sb**	**7-Bi**
Formula	$C_{42}H_{65}BiN_2SbSi$	$C_{32}H_{60}N_4Sb_2Si_2$	$C_{16}H_{30}BiN_2Si$
Formula weight, g mol^{-1}	835.03	800.52	487.49
Crystal system	Orthorhombic	Triclinic	Triclinic
Crystal size, mm	0.52 × 0.32 × 0.26	0.59 × 0.59 × 0.23	0.59 × 0.49 × 0.09
Space group	$P2_12_12_1$	P-1	P-1
a, Å	13.4794(7)	9.6926(5)	9.8084(4)
b, Å	17.0612(10)	9.9028(6)	9.9912(4)
c, Å	18.2148(8)	11.5941(7)	11.6118(4)
α, º	90	114.372(2)	114.184(2)
β, º	90	101.681(2)	100.792(2)
γ, º	90	96.559(2)	98.542(2)
V, Å^3	4188.9(4)	967.98(10)	986.96(7)
Z	4	1	2
ρ_{calcd}, Mg m^{-3}	1.324	1.373	1.640
μ (Mo $K\alpha$), mm^{-1}	4.266	1.482	1.482
F(000)	1712	410	474
θ range, deg	1 to 26.0	1 to 27.5	1 to 26.5
No. of reflns collected	33155	31488	23235
No. indep. Reflns	8201	4432	4084
No. obsd reflns with ($I>2\sigma(I)$), R_{int}	6035, 0.058	4244, 0.034	3504, 0.058
No. refined params	427	189	198
GooF (F^2)	1.067	1.144	1.145
R_1 (F) ($I > 2\sigma(I)$)	0.050	0.022	0.049
wR_2 (F^2) (all data)	0.114	0.052	0.131
Largest diff peak/hole, e Å^{-3}	1.432 / –0.986	1.822 / –0.943	2.852 / –3.532
CCDC	2203727	2203731	2203730

$R_{int} = \sum |F_o^2 - F_{o,mean}^2| / \sum F_o^2$, $S = [\sum(w(F_o^2 - F_c^2)^2)/(N_{diffrs} - N_{params})]^{1/2}$ for all data, $R(F) = \sum ||F_o| - |F_c|| / \sum |F_o|$ for observed data, $wR(F^2) = [\sum(w(F_o^2 - F_c^2)^2)/(\sum w(F_o^2)^2)]^{1/2}$ for all data.

5) IR and Raman spectra

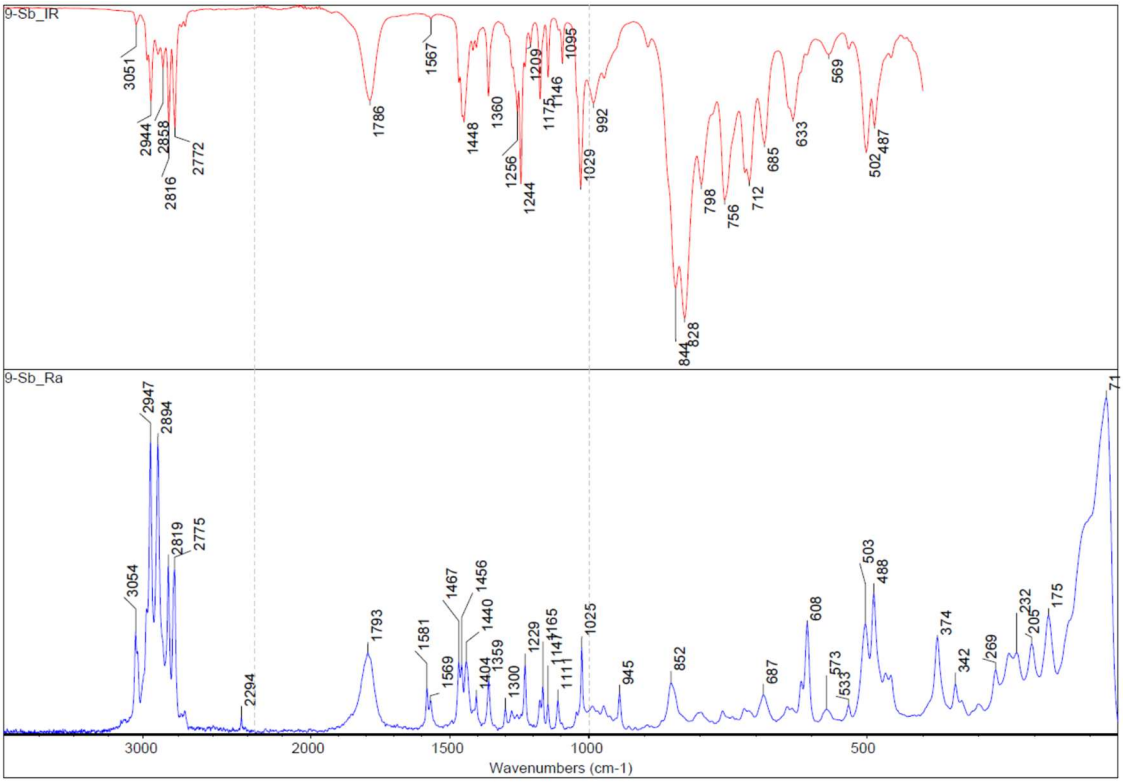

Figure S35: Infrared (top) and Raman (bottom) spectra of **9-Sb**.

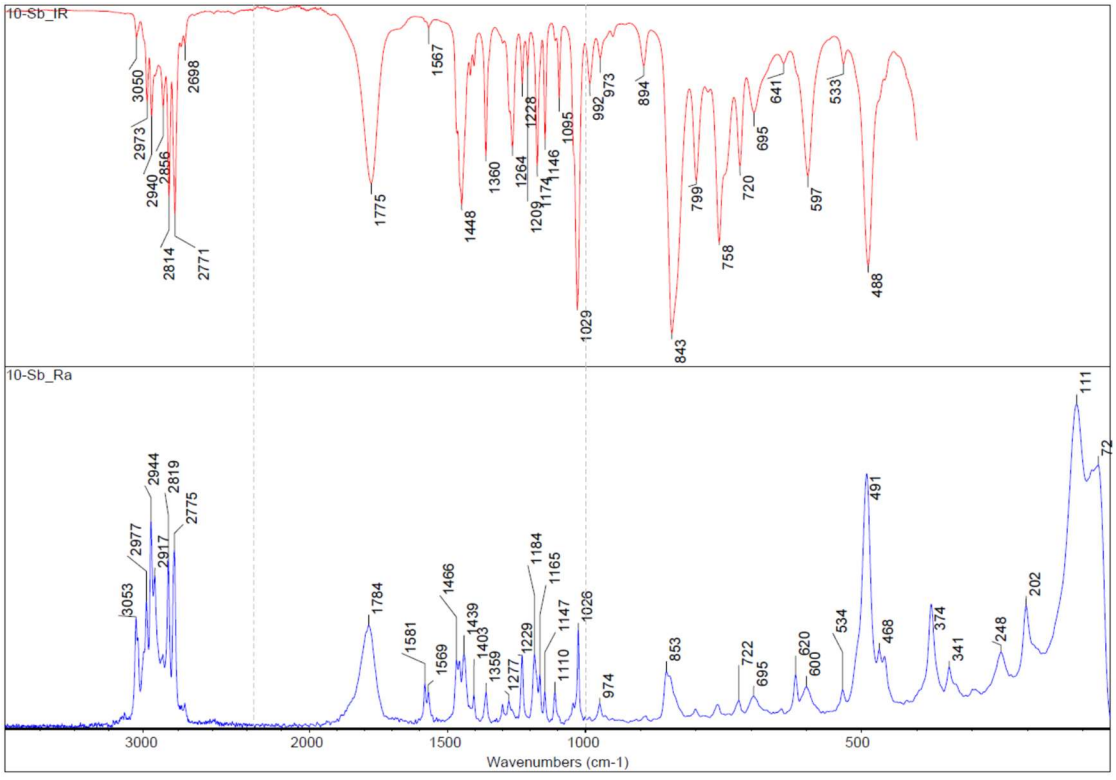

Figure S36: Infrared (top) and Raman (bottom) spectra of **10-Sb**.

6) Theoretical study

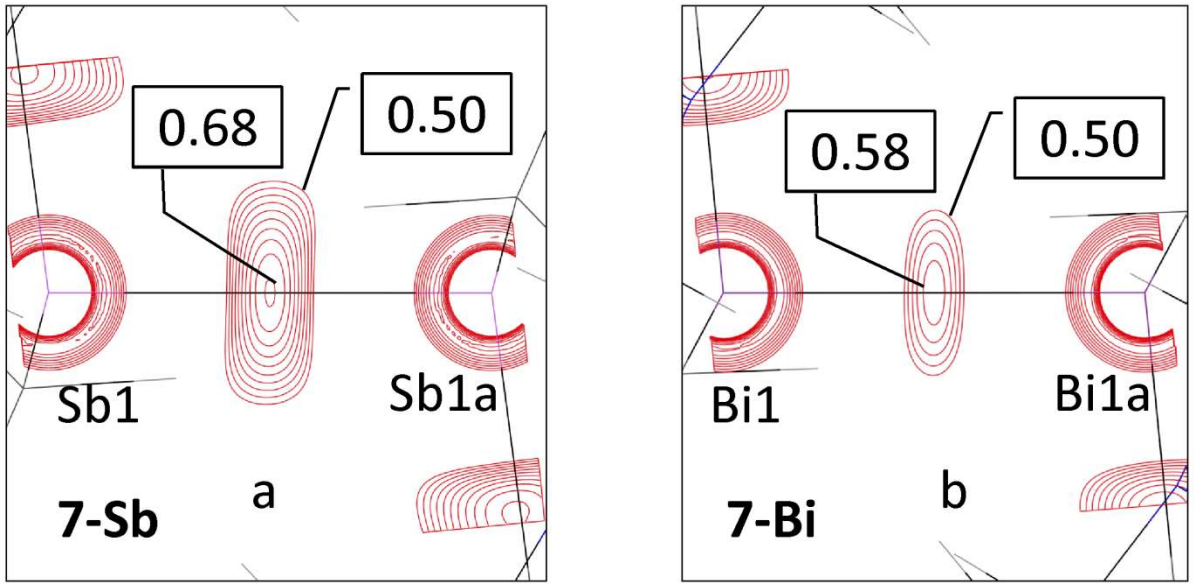

Figure S37. Contour maps of the LOL function (0.5-0.7, step 0.02) in the EEC(Arene) plane (E = Sb, Bi, Arene = [2,6-$(Me_2NCH_2)_2C_6H_3$]) of complexes *meso*-**7-Sb** (a) and *meso*-**7-Bi** (b).

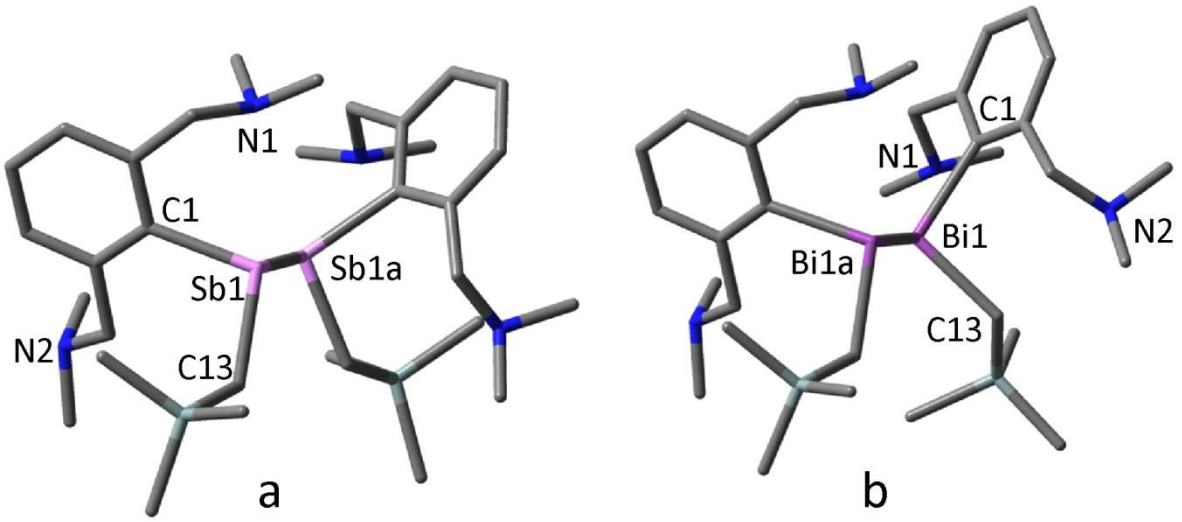

Figure S38. Optimized structures of *rac-SS*-**7-Sb** (a) and *rac-SS* **-7-Bi** (b). Hydrogen atoms are omitted for clarity. Selected bond lengths [Å] and angles [°]:*rac-SS*-**7-Sb**: Sb(1)-C(1) 2.185, Sb(1)-N(1) 3.005, Sb(1)-N(2) 4.911, Sb(1)-C(13) 2.193, Sb(1)-Sb(1a) 2.851, C(1)-Sb(1)-C(13) 102.48, C(1)-Sb(1)-Sb(1a) 92.88, C(13)-Sb(1)-Sb(1a) 99.72; *rac-SS* **-7-Bi:** Bi(1)-C(1) 2.287, Bi(1)-N(1) 3.184, Bi(1)-N(2) 4.221, Bi(1)-C(13) 2.274, Bi(1)-Bi(1a) 2.999, C(1)-Bi(1)-C(13) 100.56, C(1)-Bi(1)-Bi(1a) 98.84, C(13)-Bi(1)-Bi(1a) 94.41.

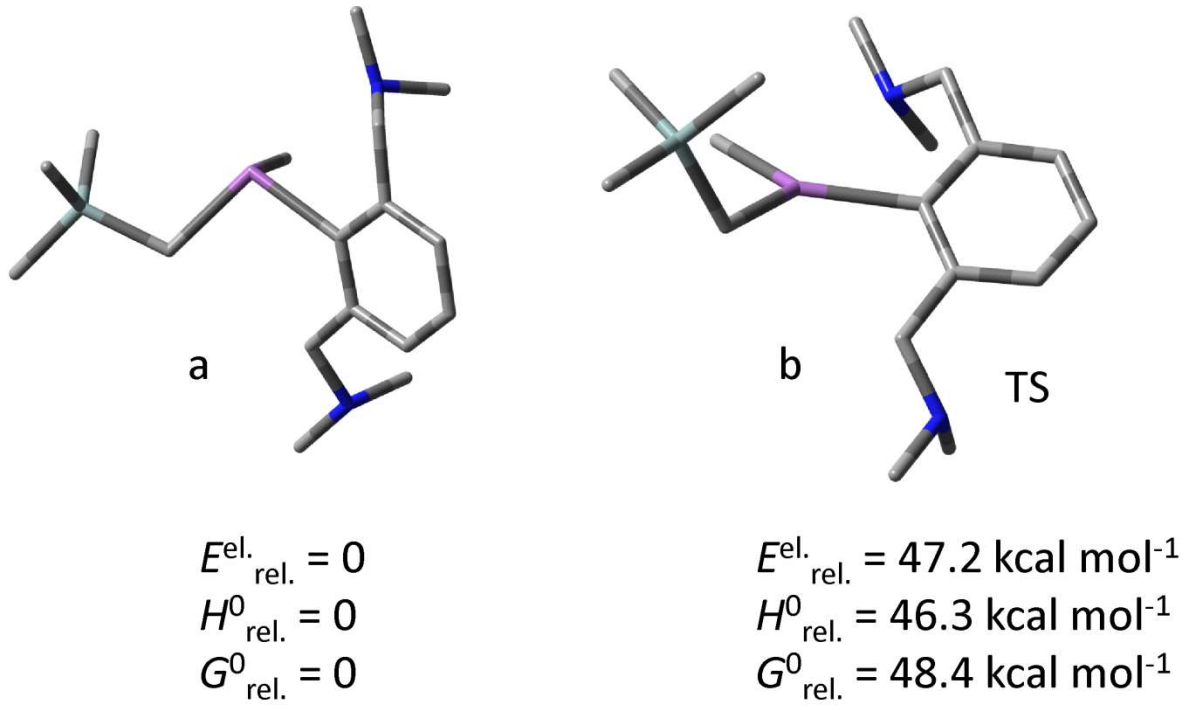

Figure S39. Optimized structures and relative energies of model complex [2,6-$(Me_2NCH_2)_2C_6H_3$](NpSi)(Me)Sb and the transition state corresponding to inversion at the Sb atom.